

Fission decay modes of $^{254}\text{Fm}^*$ compound nucleus formed in $^{16}\text{O}+^{238}\text{U}$ reaction



*European Nuclear Physics Conference 2022
(EuNPC 2022))
@ University of Santiago de Compostela,
Santiago de Compostela, Spain, October 24-28, 2022*



By:

Amandeep Kaur

Postdoctoral Researcher

Department of Physics, Faculty of Science,
University of Zagreb, Bijenička c. 32,
10000 Zagreb, Croatia

Email address: akaur.phy@pmf.hr, amanganday@gmail.com



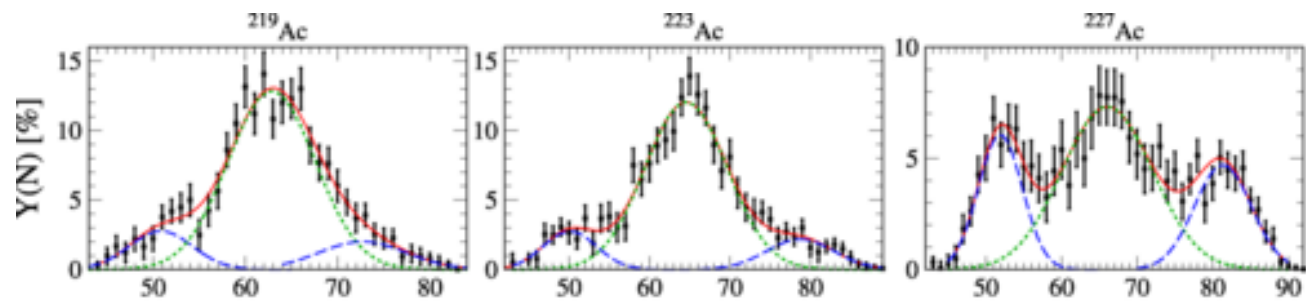
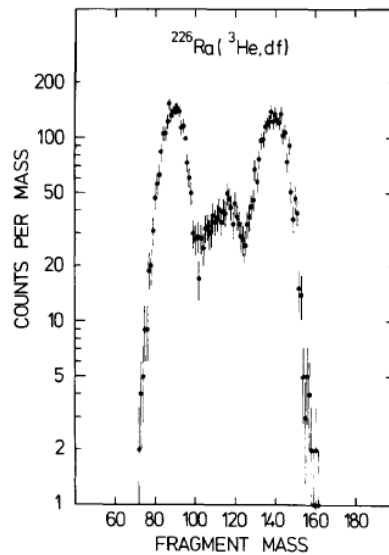
Europska unija
Zajedno do fondova EU



Operativni program
**KONKURENTNOST
I KOHEZIJA**

Introduction

- Importance of Nuclear fission:
 - Generation of energy
 - Stability of superheavy nuclei
 - Termination of the r-nucleosynthesis process
 - Generation of exotic nuclear isotopes that are useful in many industrial and medical applications.
- ^{225}Ra - ^{228}Ac nuclei exhibit two fission modes : symmetric and **asymmetric**.



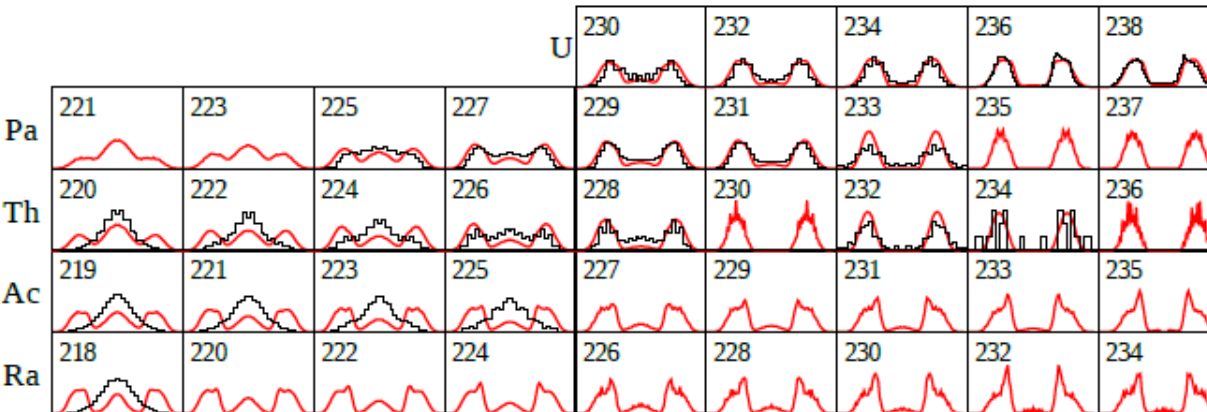
A. Chatillon et al., PRC **106**, 024618 (2022)

Fig. 1. Fragment mass distribution for fission of ^{227}Ac at excitation energies between 7 and 13 MeV.

E. Konecky et al., PLB **45**, 329 (1973)

Introduction

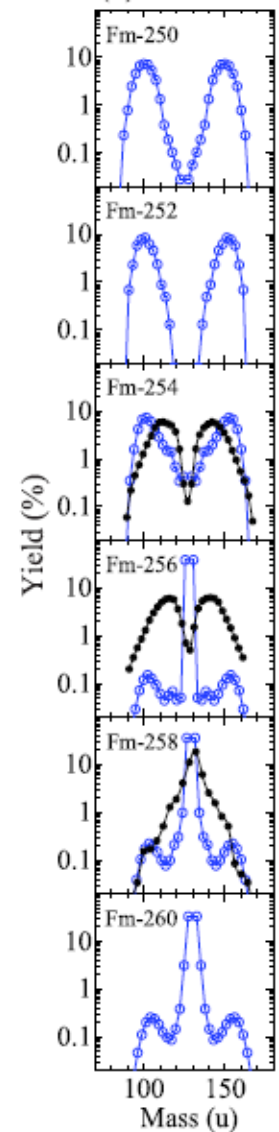
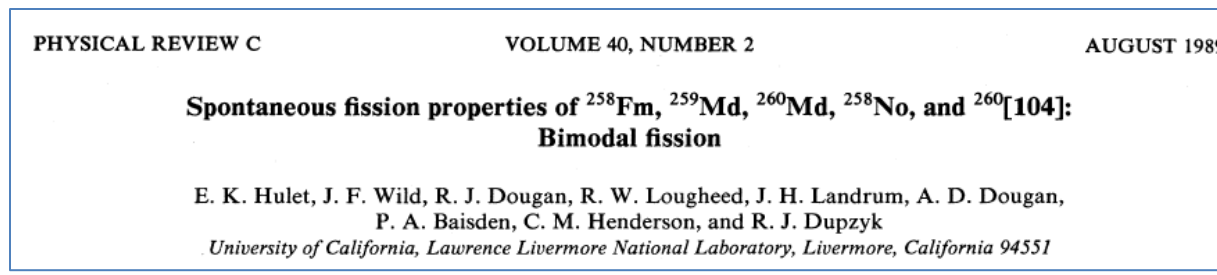
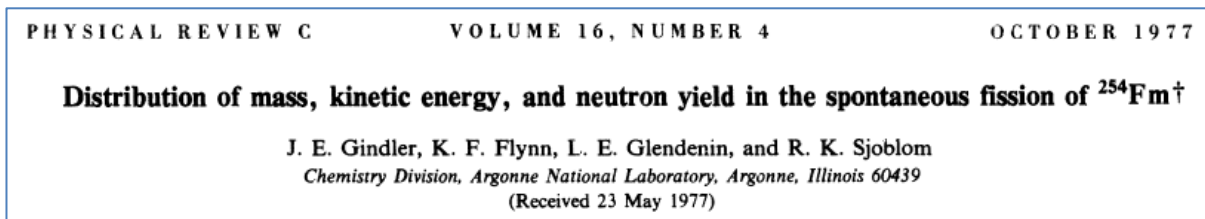
- Importance of Nuclear fission:
- Generation of energy
- Stability of superheavy nuclei
- Termination of the r-nucleosynthesis process
- Generation of exotic nuclear isotopes that are useful in many industrial and medical applications.
- **^{225}Ra - ^{228}Ac** nuclei exhibit two fission modes : symmetric and **asymmetric**.
- Generally, actinides are known to have an asymmetric fission pattern.



K. Mahata et al., PLB **825**, 136859 (2022)

Introduction

- Importance of Nuclear fission:
- Generation of energy
- Stability of superheavy nuclei
- Termination of the r-nucleosynthesis process
- Generation of exotic nuclear isotopes that are useful in many industrial and medical applications.
- ^{225}Ra - ^{228}Ac nuclei exhibit two fission modes : symmetric and **asymmetric**.
- Generally, actinides are known to have an asymmetric fission pattern.
- The first observation of a **transition from asymmetric (double humped) to symmetric spontaneous fission** has been measured in the region of mass A=254-258 of Fm isotopes.



Introduction

- Importance of Nuclear fission:
 - Generation of energy
 - Stability of superheavy nuclei
 - Termination of the r-nucleosynthesis process
 - Generation of exotic nuclear isotopes that are useful in many industrial and medical applications.
- **^{225}Ra - ^{228}Ac** nuclei exhibit two fission modes : symmetric and **asymmetric**.
- Generally, actinides are known to have an asymmetric fission pattern.
- The first observation of a **transition from asymmetric (double humped) to symmetric spontaneous fission** has been measured in the region of mass A=254-258 of Fm isotopes.
- Similar type of observations has been seen in the case of **^{254}Es** nucleus.

M. D. Usang et al., Sci. Rep. **9**, 1525 (2019).

Introduction

- Importance of Nuclear fission:
- Generation of energy
- Stability of superheavy nuclei
- Termination of the r-nucleosynthesis process
- Generation of exotic nuclear isotopes that are useful in many industrial and medical applications.
- **^{225}Ra - ^{228}Ac** nuclei exhibit two fission modes : symmetric and **asymmetric**.
- Generally, actinides are known to have an asymmetric fission pattern.
- The first observation of a **transition from asymmetric (double humped) to symmetric spontaneous fission** has been measured in the region of mass A=254-258 of Fm isotopes.
- Similar type of observations has been seen in the case of **^{254}Es** nucleus.

M. D. Usang et al., Sci. Rep. **9**, 1525 (2019).

Aim of this Work

1. To analyze the spontaneous fission decay modes of Fm isotopes.
2. To see the role of compact (side-to-side) and elongated (tip-to-tip) oriented configurations on the fission decay dynamics.
3. To investigate the possibility of multimodal fission of $^{254}\text{Fm}^*$ nucleus formed in $^{18}\text{O}+^{238}\text{U}$ reaction.
4. To study the impact of the excitation energy E^* on the fission fragment mass distribution of ^{254}Fm .

Methodology

Preformed cluster model [PCM ($\ell=0\hbar$, T=0)] and Dynamical cluster-decay model [DCM ($\ell\neq0\hbar$, T \neq 0)])

Based on quantum mechanical fragmentation theory (QMFT), which considers mass (or charge) asymmetry coordinate as a dynamical coordinate to study the mass (or charge) transfer in a nuclear decay process, PCM and DCM approach have been developed.

➤ Mass and charge asymmetry parameters

$$\eta = \frac{A_1 - A_2}{A_1 + A_2} \quad \eta_Z = \frac{Z_1 - Z_2}{Z_1 + Z_2}$$

Mass asymmetry parameter allows a unified description of a few-nucleon or multi-nucleon (a cluster) transfer and a large-mass transfer.

$$(|\eta| = 1) \quad \text{For Complete fusion}$$

$$0 \leq |\eta| \leq 1 \quad (\eta = 0) \quad \text{For symmetric fission}$$

$$0 < \eta < 1 \quad \text{For asymmetric and super asymmetric fission}$$

Methodology

Preformed cluster model [PCM ($\ell=0\hbar$, T=0)] and Dynamical cluster-decay model [DCM ($\ell\neq0\hbar$, T \neq 0)])

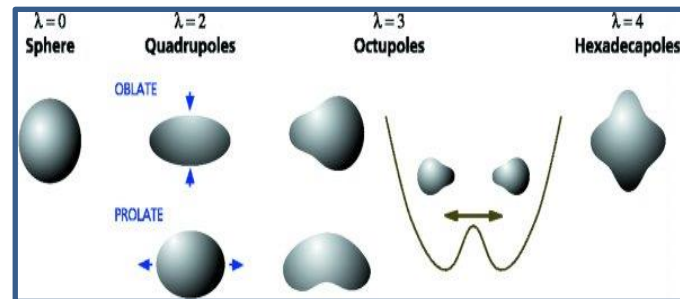
Based on quantum mechanical fragmentation theory (QMFT), which considers mass (or charge) asymmetry coordinate as a dynamical coordinate to study the mass (or charge) transfer in a nuclear decay process, DCM approach has been developed.

➤ Mass and charge asymmetry parameters

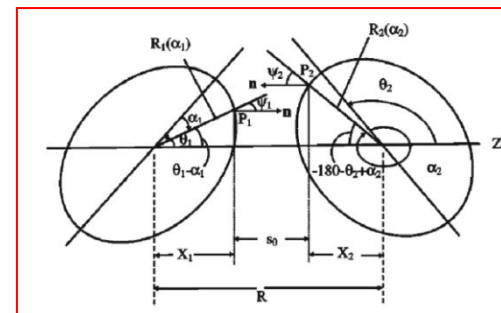
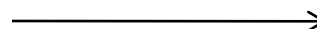
$$\eta = \frac{A_1 - A_2}{A_1 + A_2}$$

$$\eta_Z = \frac{Z_1 - Z_2}{Z_1 + Z_2}$$

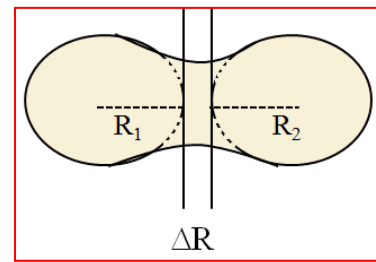
➤ The deformation co-ordinates $\beta_{\lambda i}$ ($\lambda=2,3,4..$ and $i=1,2$) fragments.



➤ The orientation degrees of freedom θ_i ($i=1,2$) of the deformed fragments.



➤ Relative separation (R).



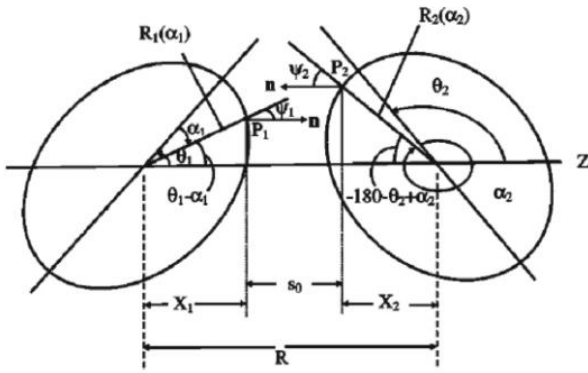
$$R = R_1 + R_2 + \Delta R$$

$$R_i(\alpha_i, T) = R_{0i}(T) \left[1 + \sum_{\lambda} \beta_{\lambda i} Y_{\lambda}^{(0)}(\alpha_i) \right],$$

$$R_{0i}(T) = \left[1.28 A_i^{\frac{1}{3}} - 0.76 + 0.8 A_i^{-\frac{1}{3}} \right] (1 + 0.0007 T^2) \text{ fm.}$$

Compact and elongated configurations

➤ The orientation degrees of freedom θ_i ($i=1,2$) of the β_2 -deformed fragments.



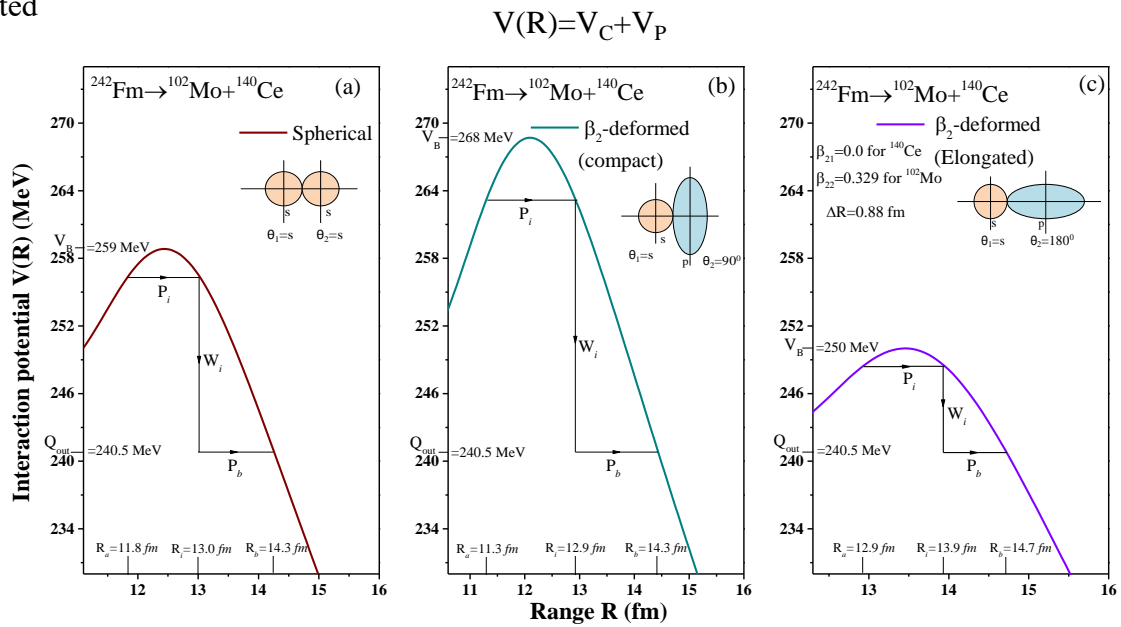
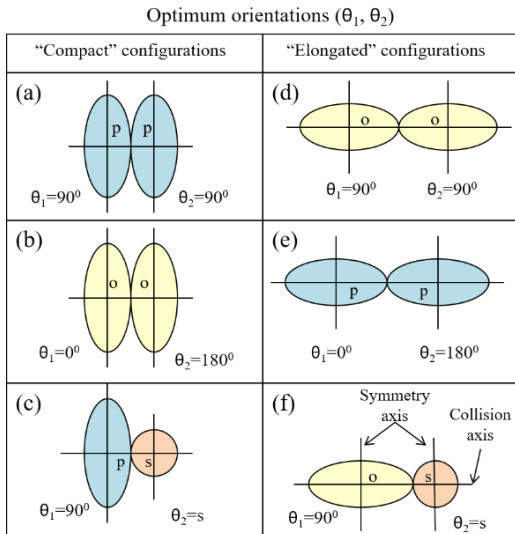
R. K. Gupta and W. Greiner *et al.*,
J. Phys. G: Nucl. Part. Phys. **31**, 631 (2005).

Optimum orientations (θ_1, θ_2)

Deformations of colliding nuclei	Elongated configuration	Compact configuration
$p^\pm p^\pm$	$0^\circ, 180^\circ$	$90^\circ, 90^\circ$
$o^\pm o^\pm$	$90^\circ, 90^\circ$	$0^\circ, 180^\circ$
$p^\pm o^\pm$	$0^\circ, 90^\circ$	$90^\circ, 180^\circ$
$o^\pm p^\pm$	$90^\circ, 180^\circ$	$0^\circ, 90^\circ$
$p^\pm s$	$0^\circ, s$	$90^\circ, s$
$o^\pm s$	$90^\circ, s$	$0^\circ, s$
sp^\pm	$s, 180^\circ$	$s, 90^\circ$
so^\pm	$s, 90^\circ$	$s, 180^\circ$

p - prolate
o - oblate
s - spherical
± - Hexadecupole

A pictorial representation of compact (a)–(c) and elongated (d)–(f) configurations for prolate (p), oblate (o), and spherical (s) shapes of nuclei.



Fragmentation potential

By using these coordinates Schrödinger equation is solved in η coordinate to find preformation probability, P_0

Schrödinger equation

$$\rightarrow \left\{ -\frac{\hbar^2}{2\sqrt{B_{\eta\eta}}} \frac{\partial}{\partial\eta} \frac{1}{\sqrt{B_{\eta\eta}}} \frac{\partial}{\partial\eta} + V_R(\eta, T) \right\} \psi^\nu(\eta) = E^\nu \psi^\nu(\eta)$$

With $\nu = 0, 1, 2, 3, \dots$
where ($\nu = 0$) refers to ground state



$$V(\eta, \eta_Z, R) = -\sum_{i=1}^2 B_i(A_i, Z_i, \beta_{\lambda i}) + V_C(R, Z_i, \beta_{\lambda i}, \theta_i, \phi) + V_\ell(R, A_i, \beta_{\lambda i}, \theta_i, \phi) + V_N(R, A_i, \beta_{\lambda i}, \theta_i, \phi)$$

Fragmentation potential

By using these coordinates Schrödinger equation is solved in η coordinate to find preformation probability, P_0

Schrödinger equation

$$\left\{ -\frac{\hbar^2}{2\sqrt{B_{\eta\eta}}}\frac{\partial}{\partial\eta}\frac{1}{\sqrt{B_{\eta\eta}}}\frac{\partial}{\partial\eta} + V_R(\eta, T) \right\} \psi^\nu(\eta) = E^\nu \psi^\nu(\eta)$$

With $\nu = 0, 1, 2, 3, \dots$
where ($\nu = 0$) refers to ground state

$$V(\eta, \eta_Z, R) = -\sum_{i=1}^2 B_i(A_i, Z_i, \beta_{\lambda i}) + V_C(R, Z_i, \beta_{\lambda i}, \theta_i, \phi) + V_\ell(R, A_i, \beta_{\lambda i}, \theta_i, \phi) + V_N(R, A_i, \beta_{\lambda i}, \theta_i, \phi)$$

The binding energy contains both the macroscopic (liquid drop model) and microscopic (shell-correction) part.

$$\sum_{i=1}^2 V_{LDM} + \sum_{i=1}^2 \delta U \exp\left(-\frac{T^2}{T_0^2}\right)$$

$$V_\ell = \frac{\hbar^2 \ell(\ell+1)}{2I(T)}$$

$$\begin{aligned} V_N(s_0) &= f(sh., geo.) \Phi(s_0) \\ &= 4\pi \bar{R} \gamma b \Phi(s_0). \end{aligned}$$

$$I(T) = I_s(T) = \mu R^2 + \frac{2}{5} A_1 m R_1^2(\alpha_1, T) + \frac{2}{5} A_2 m R_2^2(\alpha_2, T)$$

$$V_C(Z_i, \beta_{\lambda i}, \theta_i, \alpha_i, T) = \frac{Z_1 Z_2 e^2}{R(T)} + 3 Z_1 Z_2 e^2 \sum_{\lambda, i=1, 2} \frac{1}{2\lambda+1} \frac{R_i^\lambda(\alpha_i, T)}{R(T)^{\lambda+1}} Y_\lambda^{(0)}(\theta_i) \left[\beta_{\lambda i} + \frac{4}{7} \beta_{\lambda i}^2(\theta_i) \right]$$

In PCM, the T and ℓ -effects are silent.

Preformation probability P_0

By using these coordinates Schrödinger equation is solved in η coordinate to find preformation probability, P_0

Schrödinger equation

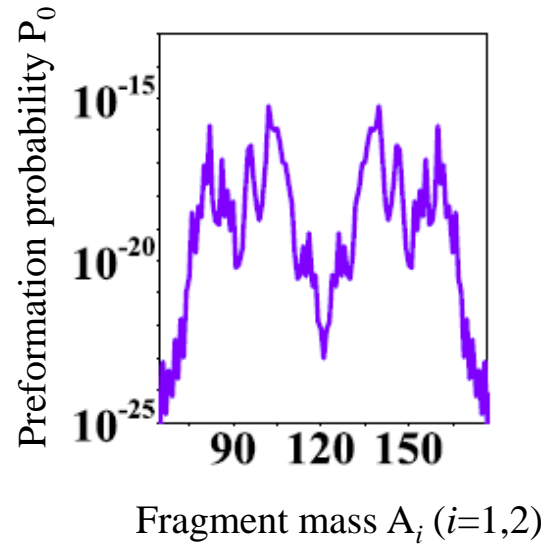
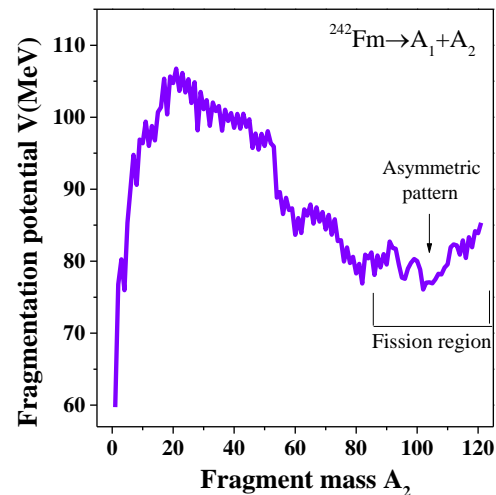
$$\rightarrow \left\{ -\frac{\hbar^2}{2\sqrt{B_{\eta\eta}}} \frac{\partial}{\partial\eta} \frac{1}{\sqrt{B_{\eta\eta}}} \frac{\partial}{\partial\eta} + V_R(\eta, T) \right\} \psi^\nu(\eta) = E^\nu \psi^\nu(\eta)$$

With $\nu = 0, 1, 2, 3, \dots$
where ($\nu = 0$) refers to ground state

Preformation Probability

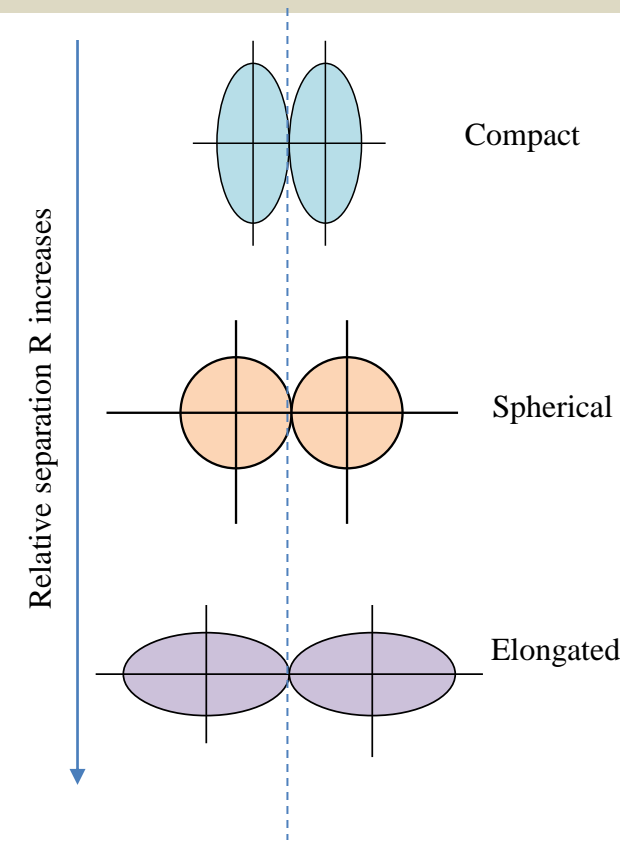
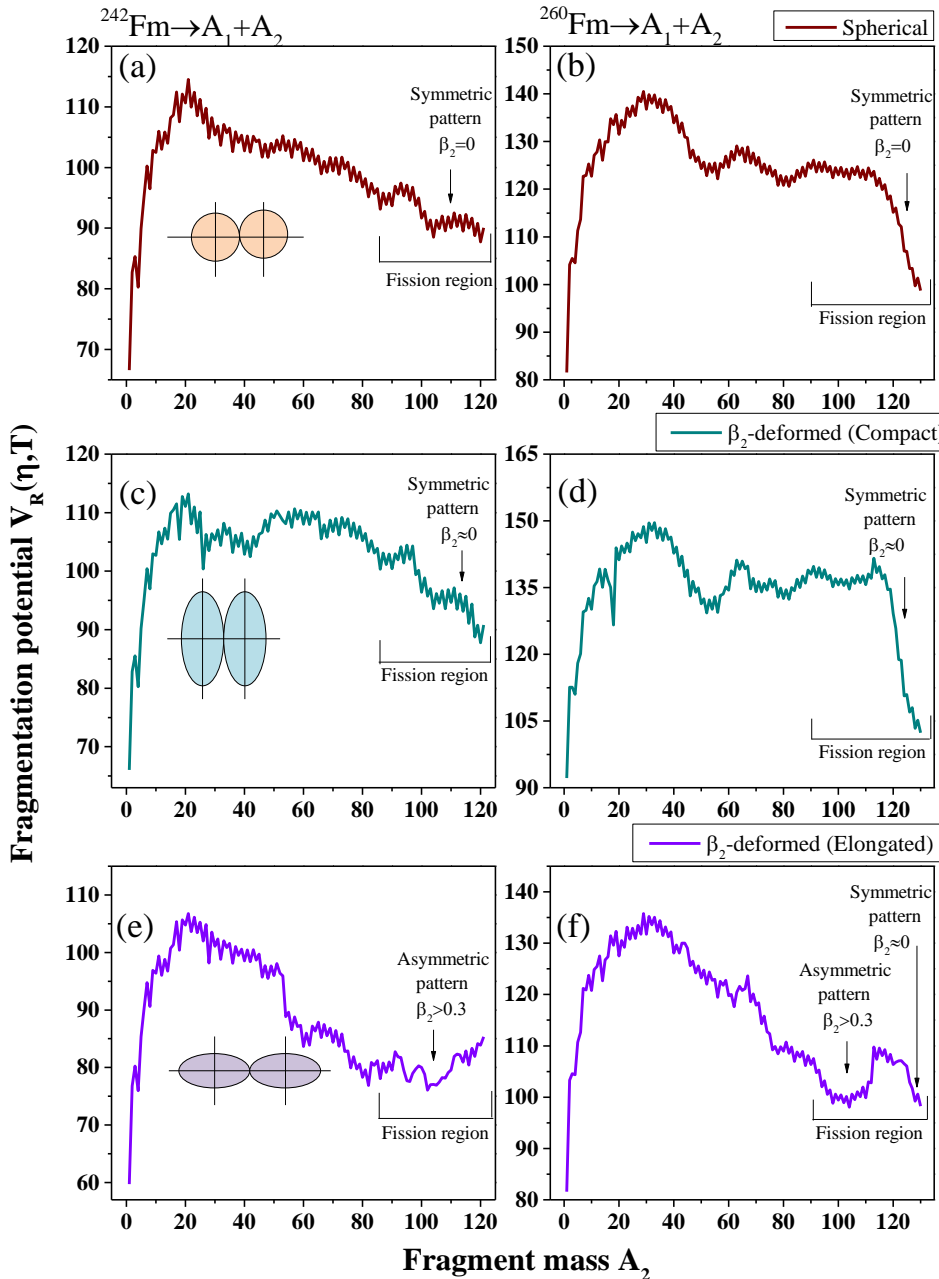
$$\rightarrow P_0 = \sqrt{B_{\eta\eta}} |\Psi[\eta(A_i)]|^2 \left(\frac{2}{A} \right)$$

Solution

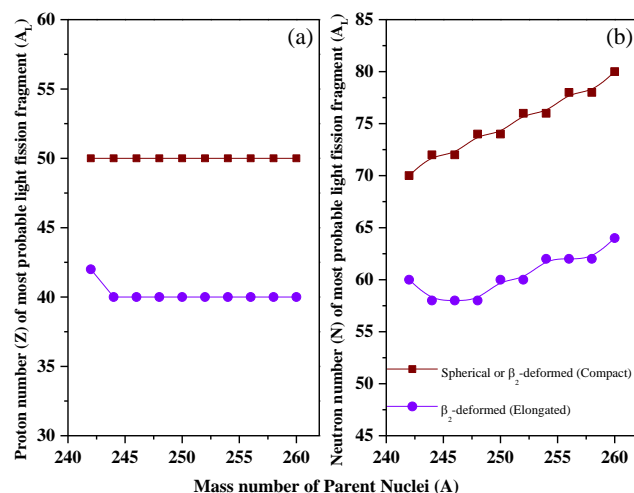
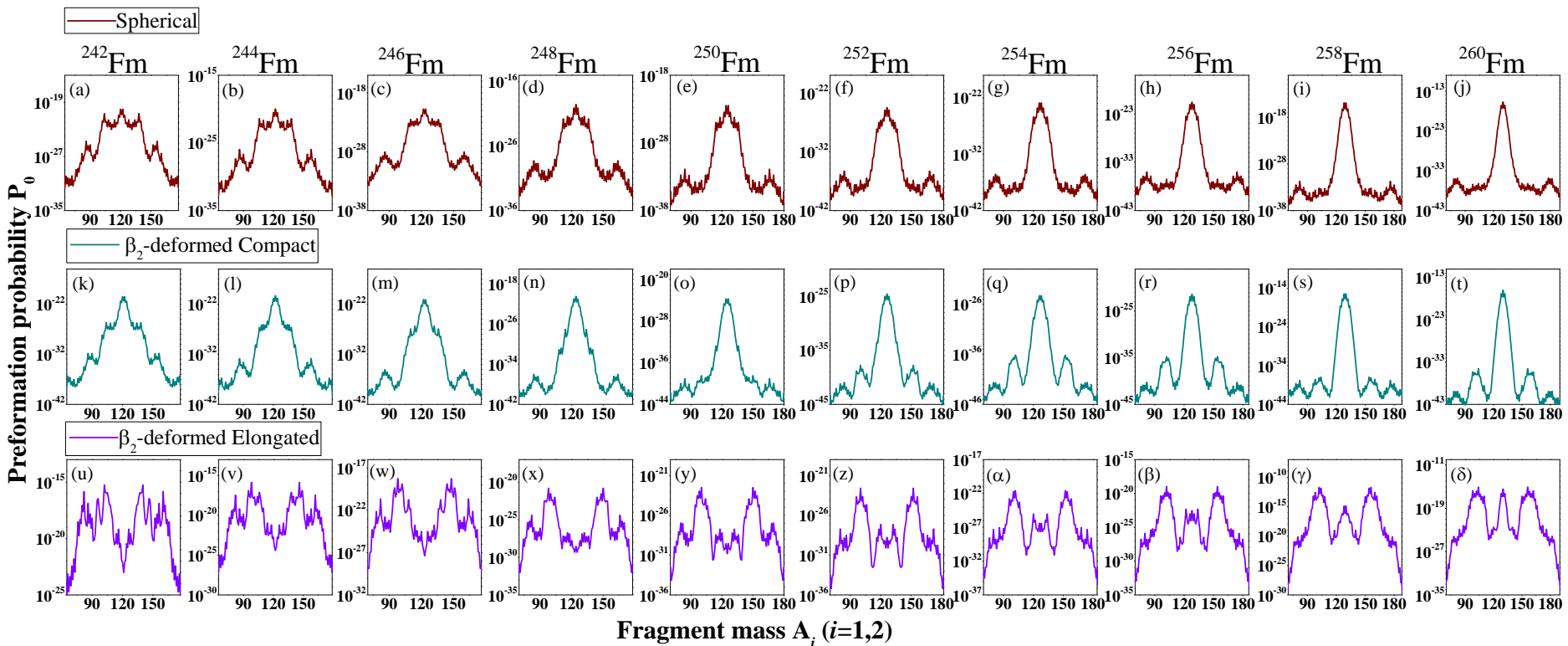


Spontaneous fission of Fm isotopes with mass A=242-260

Using PCM..

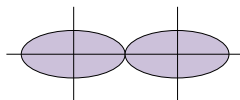


Spontaneous fission of Fm isotopes with mass A=242-260

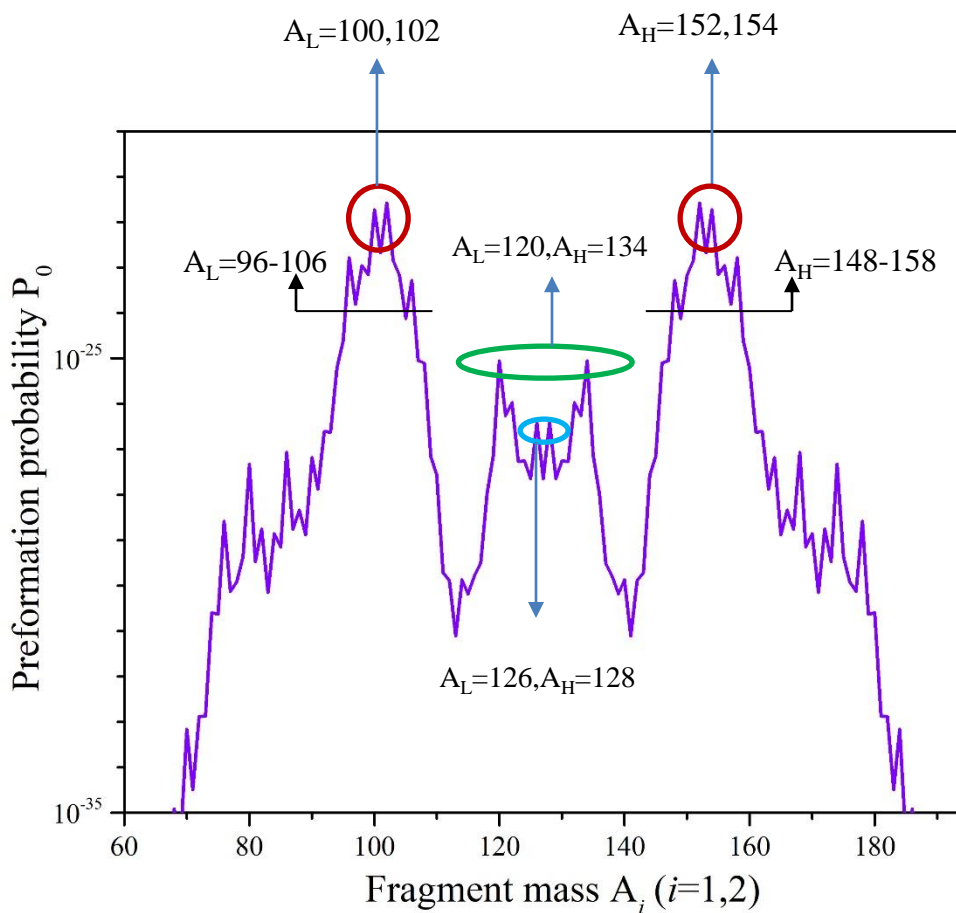


Spontaneous fission of ^{254}Fm

Elongated configurations



A_H	$\beta_2(H)$	A_L	$\beta_2(L)$
$^{128}\text{Sn} (Z=50, N=78)$	0.0	$^{126}\text{Sn} (Z=50, N=76)$	0.0
$^{134}\text{Te} (Z=52, N=82)$	0.0	$^{120}\text{Cd} (Z=48, N=72)$	0.024
$^{154}\text{Nd} (Z=60, N=92)$	0.048	$^{100}\text{Zr} (Z=40, N=62)$	0.064

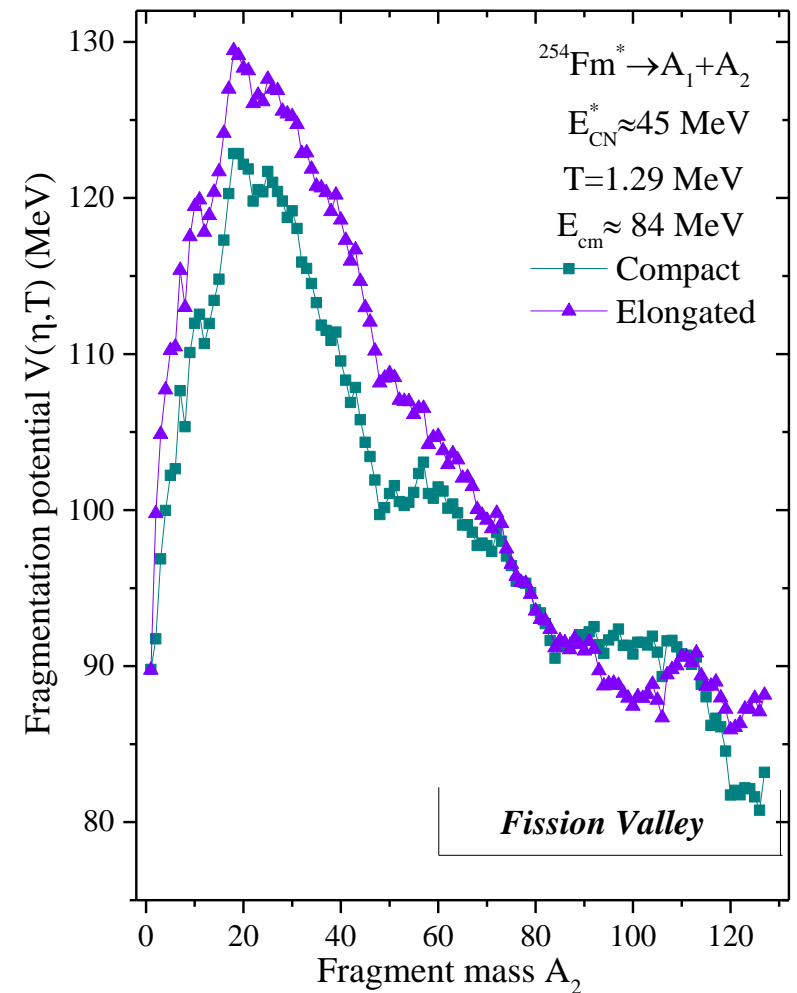


Experimental paper
T. Banerjee et al.,
PRC **105**, 044614 (2022)

$\tilde{\chi}^2$	Mode	$\langle M_H \rangle$ (u)
0.64 (mass fit)	SL	127.0^\dagger
1.46 (TKE fit)		
(mass fit)	S1	134.80 ± 1.94
(TKE fit)		134.80^\dagger
(mass fit)	S2	141.95 ± 1.37
(TKE fit)		141.95^\dagger
(mass fit)	S3	154.92 ± 4.79
(TKE fit)		154.92^\dagger

Fission decay modes of $^{254}\text{Fm}^*$ compound nucleus formed in $^{16}\text{O} + ^{238}\text{U}$ reaction

Preliminary results calculated using DCM



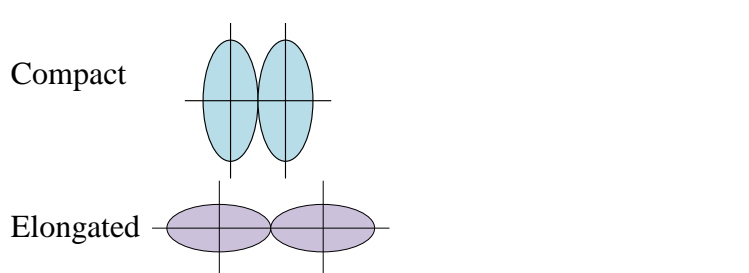
The deformation parameters are also made T-dependent:

$$\beta_{\lambda i}(T) = \exp(-T/T_0) \beta_{\lambda i}(0),$$

$\beta_{\lambda i}(0)$ = static deformation

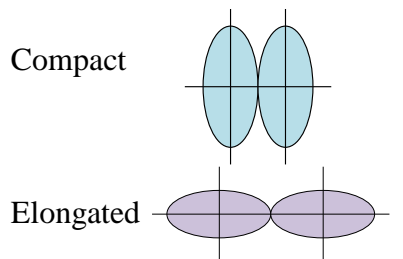
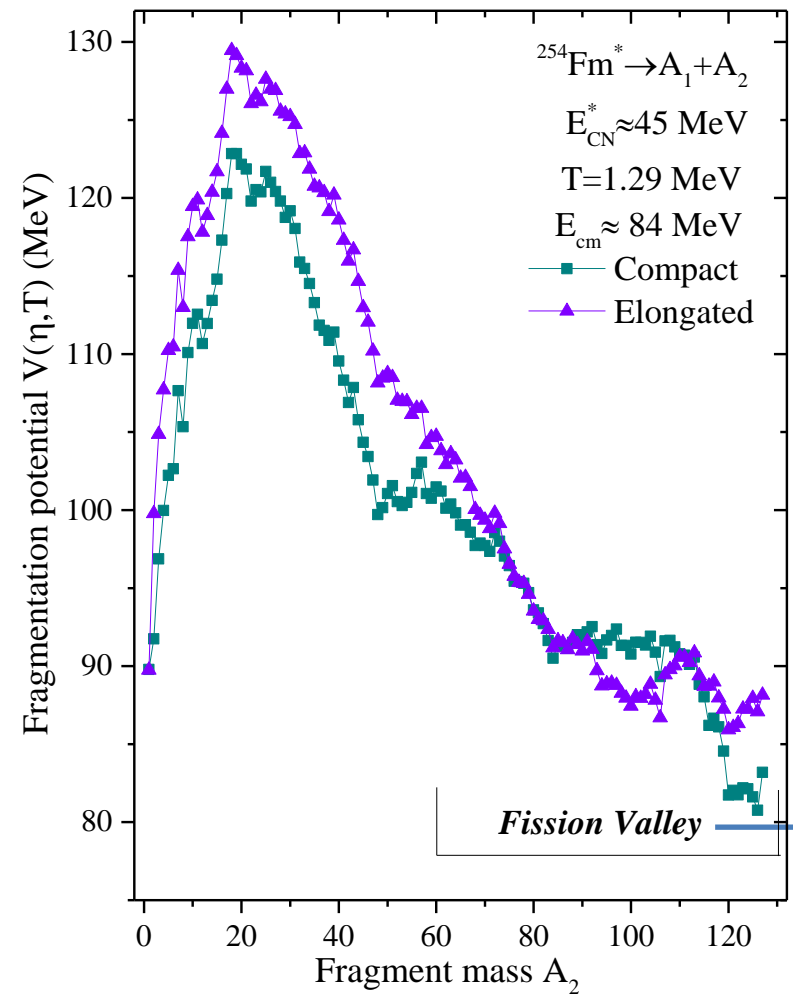
$T_0 = 1.5 \text{ MeV}$ at which shell effects start to vanish

M. Rashdan, A. Faessler, and W. Waid, J. Phys. G: Nucl. Part. Phys. **17**, 1401 (1991).



Fission decay modes of $^{254}\text{Fm}^*$ compound nucleus formed in $^{16}\text{O} + ^{238}\text{U}$ reaction

Preliminary results calculated using DCM



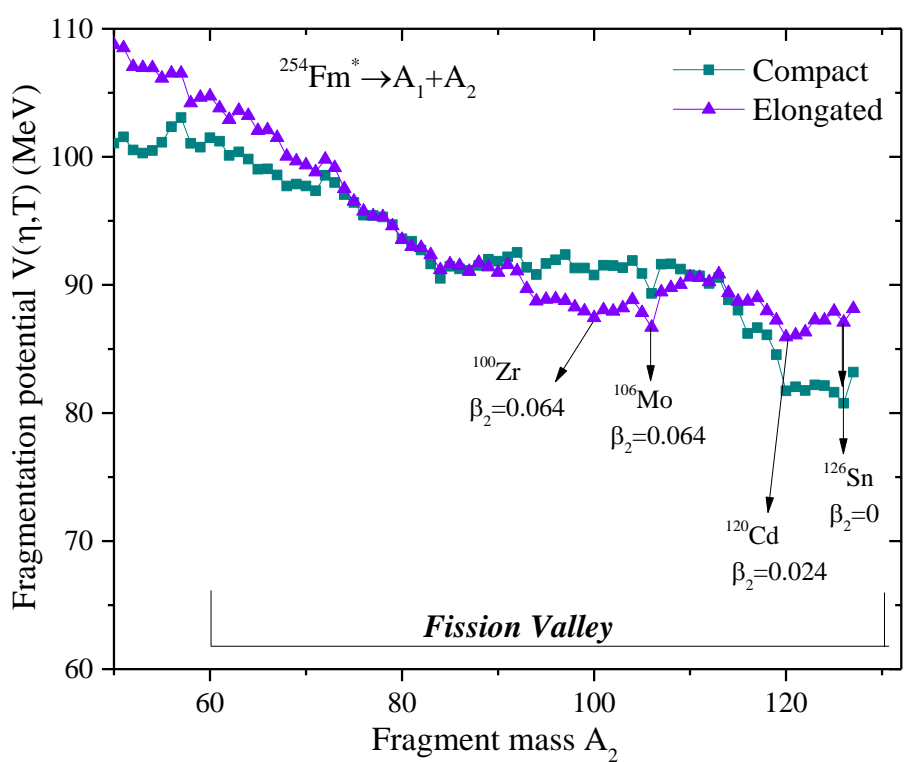
The deformation parameters are also made T-dependent:

$$\beta_{\lambda i}(T) = \exp(-T/T_0)\beta_{\lambda i}(0),$$

$\beta_{\lambda i}(0)$ = static deformation

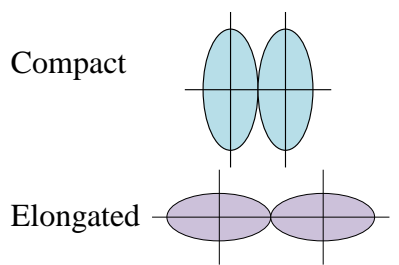
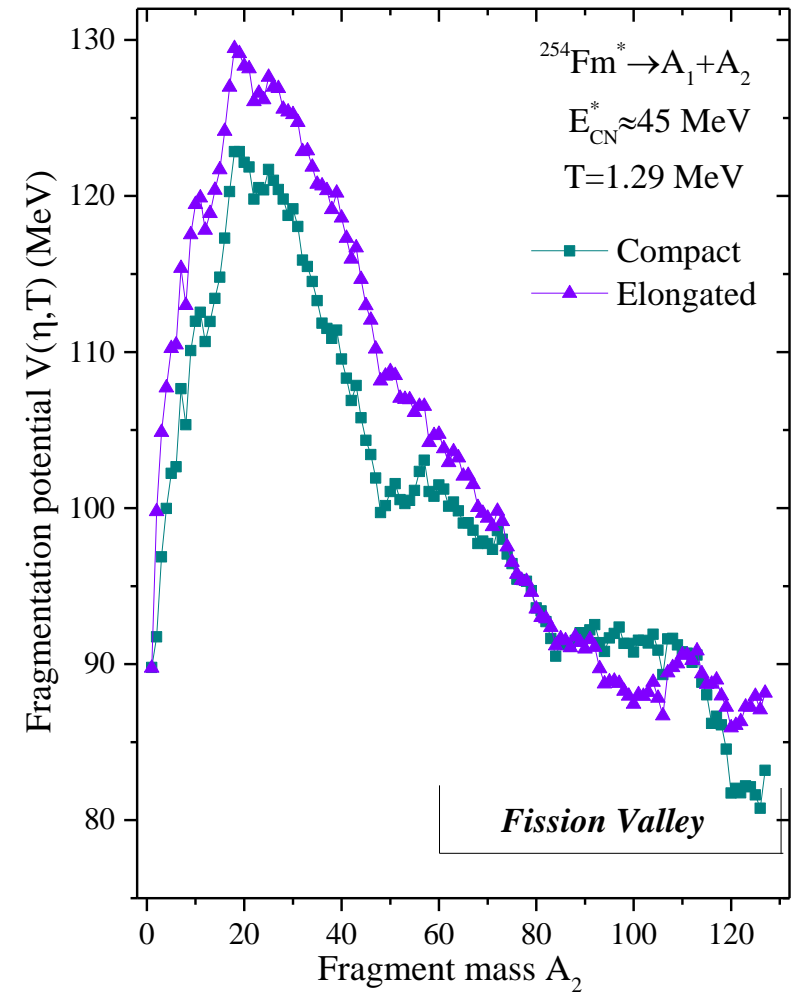
$T_0 = 1.5 \text{ MeV}$ at which shell effects start to vanish

M. Rashdan, A. Faessler, and W. Waid, J. Phys. G: Nucl. Part. Phys. **17**, 1401 (1991).



Fission decay modes of $^{254}\text{Fm}^*$ compound nucleus formed in $^{16}\text{O} + ^{238}\text{U}$ reaction

Preliminary results calculated using DCM



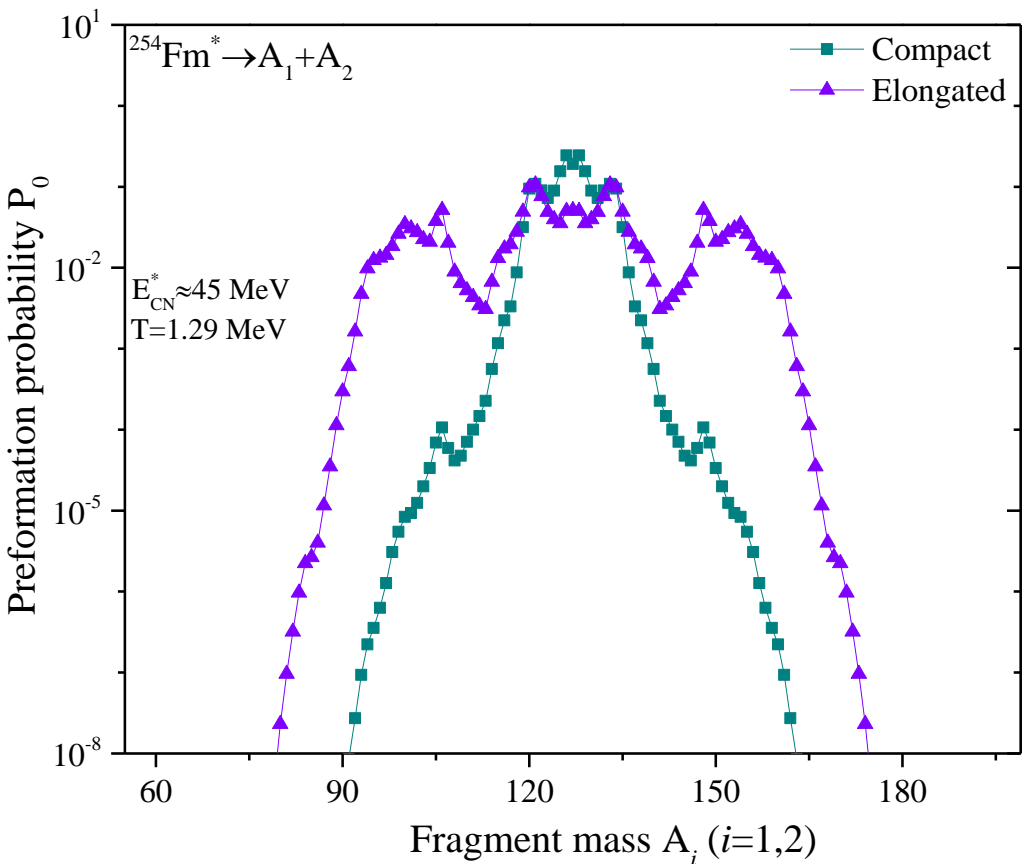
The deformation parameters are also made T-dependent:

$$\beta_{\lambda i}(T) = \exp(-T/T_0)\beta_{\lambda i}(0),$$

$\beta_{\lambda i}(0)$ = static deformation

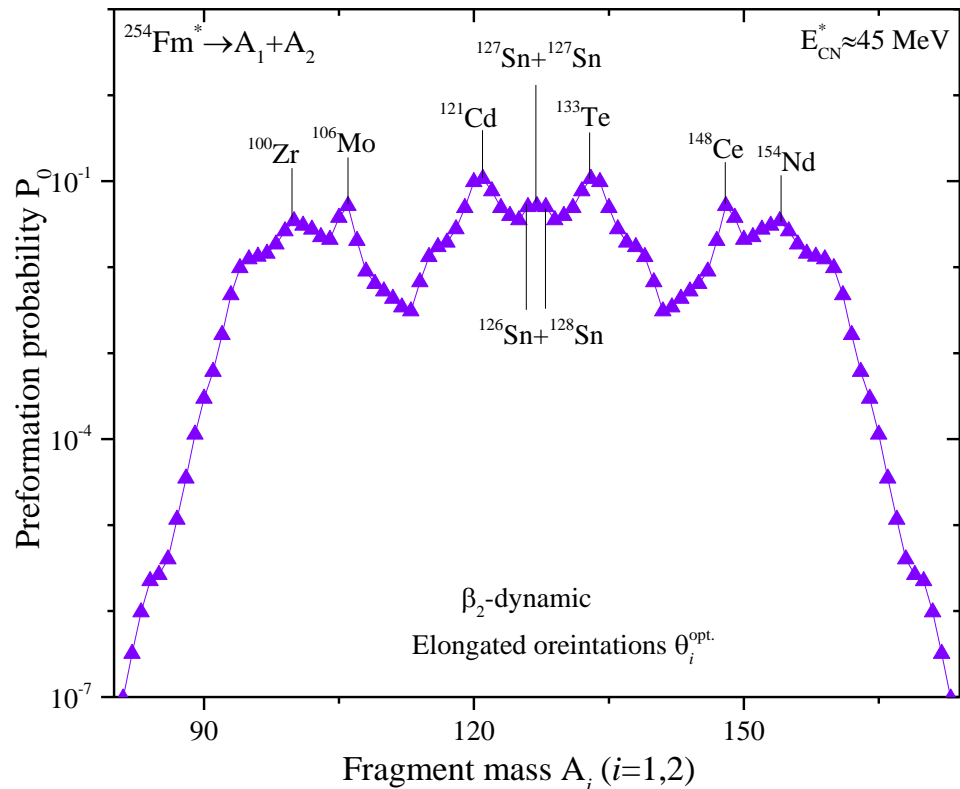
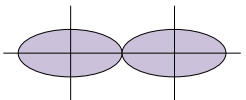
$T_0 = 1.5 \text{ MeV}$ at which shell effects start to vanish

M. Rashdan, A. Faessler, and W. Waid, J. Phys. G: Nucl. Part. Phys. **17**, 1401 (1991).



Fission decay modes of $^{254}\text{Fm}^*$ compound nucleus formed in $^{16}\text{O}+^{238}\text{U}$ reaction

Elongated configuration



Identification of A_H and A_L fragments

Fission Mode	Heavy mass fission fragment (A_H)	Light mass fission fragment (A_L)
Symmetric Superlong (SL)	$^{127}\text{Sn} (Z_H=50, N_H=77) (\beta_2=0)$	$^{127}\text{Sn} (Z_L=50, N_L=77) (\beta_2=0)$
	$^{127}\text{Sn} (Z_H=50, N_H=78) (\beta_2=0)$	$^{126}\text{Sn} (Z_L=50, N_L=76) (\beta_2=0)$
Asymmetric Standard 1 (S1)	$^{133}\text{Te} (Z_H=52, N_H=81) (\beta_2=0.001)$	$^{121}\text{Cd} (Z_L=48, N_L=73) (\beta_2=0.024)$
Asymmetric Standard 2 (S2)	$^{148}\text{Ce} (Z_H=58, N_H=90) (\beta_2=0.038)$	$^{106}\text{Mo} (Z_L=42, N_L=64) (\beta_2=0.064)$
	$^{154}\text{Nd} (Z_H=60, N_H=76) (\beta_2=0.048)$	$^{100}\text{Zr} (Z_L=40, N_L=60) (\beta_2=0.064)$

E^* (MeV)	$\tilde{\chi}^2$	Mode	$\langle M_i \rangle$ (u)
45	1.01	SL	127.0 [†]
		S1	135.0 [†]
		S2	143.0 [†]

SL = two spherical fragments ($Z=50$)

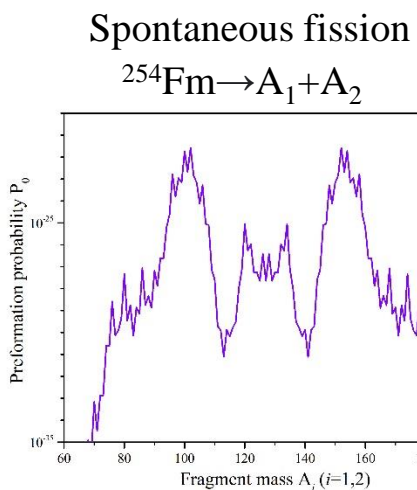
S1 = one spherical heavy fragment and a deformed light fragment ($Z=50, N=82$)

S2 = two moderately deformed fragments ($N=60, 88, Z=38$)

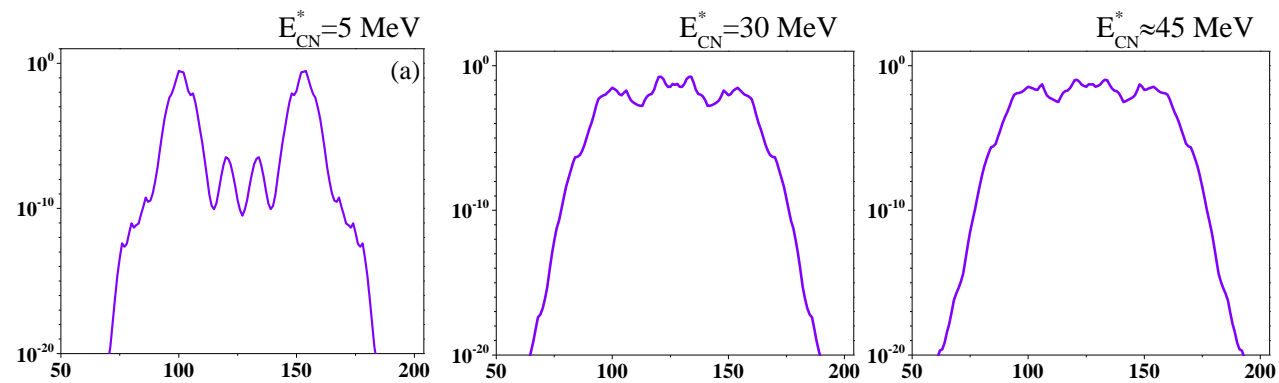
Experimental paper:

T. Banerjee et al., PRC **105**, 044614 (2022)

Energy dependence of fission fragment mass distributions



Fusion-fission $^{254}\text{Fm}^* \rightarrow \text{A}_1 + \text{A}_2$



A. Kaur et al., PRC **103**, 034618 (2021)

Summary

- Elongated configurations represent better results in terms of fission fragment mass distributions as compared to the compact orientations.
- Spherical/deformed magic shell closures and the excitation energy of compound nucleus play significant role in the division of fissioning nuclei.
- It would be interesting to include the pear shaped deformations in the decaying fragments to analyse the possible fission modes of $^{254}\text{Fm}^*$ and of other nuclei in this mass region. Also, the TKE of each fission mode will be investigated.

Acknowledgement

This work was supported by the QuantiXLie Centre of Excellence, a project co-financed by the Croatian Government and European Union through the European Regional Development Fund - the Competitiveness and Cohesion Operational Program (Grant KK.01.1.1.01.0004).

For more information please visit:
<http://bela.phy.hr/quantixlie/hr/>
<https://strukturnifondovi.hr/>

The sole responsibility for the content of this presentation lies with the Faculty of Science, University of Zagreb. It does not necessarily reflect the opinion of the European Union.



Europska unija
Zajedno do fondova EU



Operativni program
**KONKURENTNOST
I KOHEZIJA**

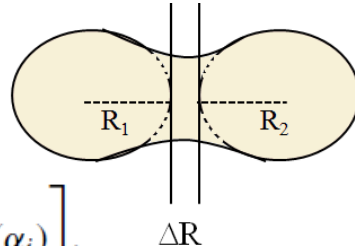
Methodology

Penetrability (P) is calculated by using WKB method as follows:

$$P = \exp\left[-\frac{2}{\hbar} \int_{R_a}^{R_b} \{2\mu[V(R) - Q_{eff}]\}^{1/2} dR\right]$$

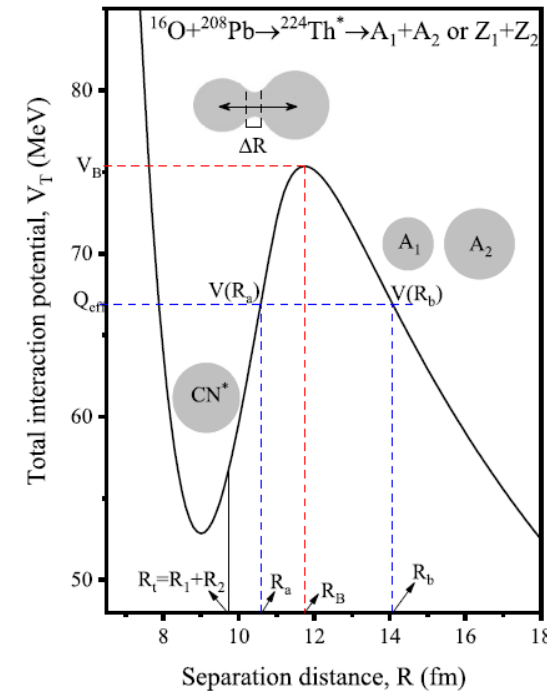
where R_a and R_b are the two turning points of WKB integral. R_a is defined as

$$R_a = R_1 + R_2 + \Delta R$$



$$R_i(\alpha_i, T) = R_{0i}(T) \left[1 + \sum \beta_{\lambda i} Y_{\lambda}^{(0)}(\alpha_i) \right],$$

$$R_{0i}(T) = \left[1.28A_i^{\frac{1}{3}} - 0.76 + 0.8A_i^{-\frac{1}{3}} \right] (1 + 0.0007T^2) \text{ fm.}$$



In DCM, after getting Preformation and penetrability, for ℓ -partial wave analysis, the decay cross-sections for each fragmentation is defined as:

Decay Cross-Section (σ) in terms of ℓ -partial waves is given as follows:



$$\sigma(A_1, A_2) = \frac{\pi}{k^2} \sum_{\ell=0}^{\ell_{max}} (2\ell+1) P_0 P$$

$$k = \sqrt{\frac{2\mu E_{c.m.}}{\hbar^2}}$$

In PCM, the decay half-life $T_{1/2}$ and the decay constant λ are calculated as

$$T_{1/2} = \frac{\ln 2}{\lambda} = v P_0 P.$$

v_0 is the barrier assault frequency, calculated as

$$v_0 = \frac{\text{velocity}}{R_0} = \frac{(2E_2/\mu)^{1/2}}{R_0}$$